

# Geometry optimization, factors screening, and introduce a predicting mathematical model of inhalation exposure chamber's performance.

**Hassan Rajabi-Vardanjani**

Tarbiat Modares University

**Hassan Asilian-Mahabadi** (✉ [asilia\\_h@modares.ac.ir](mailto:asilia_h@modares.ac.ir))

Tarbiat Modares University <https://orcid.org/0000-0001-7959-8065>

**Morteza Bayareh**

Shahrekord University of Medical Science

**Morteza Sedehi**

Shahrekord University of Medical Science

---

## Research

**Keywords:** Exposure chamber, Optimization, Modeling, Inhalation exposure

**Posted Date:** January 7th, 2020

**DOI:** <https://doi.org/10.21203/rs.2.20195/v1>

**License:**  This work is licensed under a Creative Commons Attribution 4.0 International License.

[Read Full License](#)

---

# Abstract

**Background** Optimizing the geometry of an inhalation exposure chamber (IEC) results in a uniform and stable distribution of the test atmosphere and enables the modeling of its performance. This study was conducted for the first time to optimize and model the performance of an IEC.

**Methods** The current study was performed on the initial design of the ASRA chamber and to optimize and model it. The matrix of experiments was determined by the design expert software (DE7). The mean of particle concentration (MPC) in the respiratory zone of animals as the response variable, and height of the cylindrical section of the chamber, carrier gas density, inlet concentration, and particle aerodynamic diameter (  $d_a$  ) as independent variables were considered. Experiments were performed by numerical simulation using ANSYS Workbench package. Particle concentration sampling was measured in 40 points at the opening of each holder in CFD-Post software. To determine the optimal range of the chamber's height, the different of MPC among the holders' opening was investigated by the ANOVA test. The final mathematical model was achieved by analyzing the response variables in DE7.

**Results** Thirty designs in five geometries with different heights were introduced as the matrix of experiments by DE7. The optimal height was obtained 2-2.5 times the radial of the cylindrical section. Analysis of the results suggested a linear model (2FI) with coefficients of recognition higher than 99%. The final model was significant with the presence of the inlet concentration and  $d_a$  . Gas density and height had no significant effect and were removed (  $P > 0.05$  ).

**Conclusion** The optimization of the geometry of the ASRA chamber resulted in a uniform and stable distribution of the particles and provided an accurate mathematical model to predict the particle concentration in the target zone.

# Background

In toxicological studies of gases and particulate matters carried out on laboratory animals or humans, providing uniform and stable distribution of the test atmosphere (TM) is one of the primary requirements. Researchers use inhalation exposure chambers (IEC) to evaluate the physiological effects of TM [1, 2]. The designing, construction, and application of these chambers require knowledge and experience in chamber technology and the principles of generation and analysis of TM [2]. The heterogeneous distribution of TM in the exposure chamber results in temporal and spatial variations in TM concentration and can expose a group under study to heterogeneous concentrations, therefore in interpreting dose-response results, the overestimation or underestimation of toxicity of TM may be attributed to the target concentration [3]. The uniformity of TM distribution in exposure chambers depends on several factors such as chamber geometry, flow type, particle size, and particle density [2, 4–6], which should be taken into account in designing exposure chambers. Most existing exposure chambers are designed in such a way that by changing the conditions of the test, and material, as well as by changing the animal and its location, it is necessary to examine the possible variation in concentration in the respiratory zone of

laboratory animals. The studies of Kimmel *et al.* [7] and Oldham *et al.* [8] are among the most comprehensive investigations of exposure chamber design. However, the results of these studies show concentration variations of the particles in different points of the chambers. There is also no model to predict the performance of these chambers under different conditions.

In 2018, the initial geometry of the ASRA chamber was determined after conducting a systematic review[2]. This chamber was designed as a whole-body (WB) inhalation chamber type and specific to expose small laboratory animal with suspended particles. In the ASRA chamber, the respiratory zone of the animal under study is kept constant by specific restrainers and holders, and the thermal stress in the nose-only chambers can be reduced depending on the location of the animals in the internal atmosphere of the chamber [9]. In this chamber, it is possible to create a steady flow and uniform distribution of the test atmosphere in the respiratory zone of the animals under test, and subsequently, it is possible to optimize and model the performance of this chamber. So far, optimization, screening for effective factors on the performance of the exposure chambers, and modeling of them have not been carried out; therefore, available chambers are valid only under certain conditions of the same studies. The current study aims to optimize the initial design of the ASRA exposure chamber's geometry, to screen for effective factors, and to present a specific mathematical model to predict the MPC.

## Methods

### Characteristics of the ASRA chamber geometry

The ASRA exposure chamber has an exposure (cylindrical) section, upper and lower cones as Inlet and outlet of flow. It has a metal perforated plate as a diffuser. The radius of the exposure section is 36 cm and the range of variations in its height was predicted up to 3 times the radius. The inlet and outlet radius are considered to be one-fifth of the exposure section's radius. The upper cone has an angle of 45° and the lower cone has an angle of 60°. The metal diffuser with 2 mm thickness is located on the upper part of the chamber's cylindrical section and has pores of 8 mm in diameter. In the ASRA chamber, six holders were designed to fix the animals (mouse or rat) in the exposure section. After placing the animal in the holders, its head will be positioned toward the central axis of the chamber. The distance of the holders' opening to the chamber's central axis is 10 cm, and the angle between the two adjacent holders is 60° [9].

### Characteristics of the flow and TM

The fluid flow in this chamber is of a two-phase and incompressible type. The fluid flow is turbulent because of the presence of diffusers and holders in the chamber. The air as the continuous phase and carrier gas, and the inhalable particles as discrete phase were present. Based on the particles larger than PM<sub>10</sub> are filtered through the nasal cavity, they do not pose a serious health risk [10], so in the current study, the particles with an aerodynamic diameter of 0.1-10 µm, at the concentrations of 1-45 mg/m<sup>3</sup> were used (inert and mono-dispersed). Air exchange was considered 12 times per hour [2, 9, 6, 11] and the

velocity of the inlet flow was calculated based on the volume of the chambers, flow rate and the inlet's cross-section in each chamber design.

#### Geometry optimization, factors screening and modeling

Design of experiments (DOE) method and more specifically the *Response Surface Methodology-Central Composite Design* (RSM-CCD) in DE7 software was used to determine the matrix of experiments, screen for factors, and mathematical modeling. The matrix of experiments is deliberately and purposefully determined so that the least experiments will be performed to predict the level of the response variable [12]. The height of the cylindrical section of the ASRA chamber was selected as one of the possible effective factors on the uniform distribution of the particles in the animal's respiratory zone (as an independent factor) because the height of the cylindrical section is the most important factor to create a developed flow[2]. In the continuous phase domain, the flow velocity and the density of the carrier gas, and in the discrete phase domain, the aerodynamic diameter and inlet concentration of the particles were selected as other independent factors[9]. The MPC of the respiratory zones was considered as the response variable. After determining the matrix, the experiments were performed by numerical simulation using *ANSYS FLUENT* software. The results (MPCs) were entered in DE7 software. Factors screening was done as stepwise and the final model was determined. The goodness of model was evaluated using *R-squares* and *adequate precision* indices. Also, to determine the permissible tolerance of the chamber's height, the difference in MPC at the openings of the holders (for each chamber separately) was investigated using the *ANOVA* test in *SPSS22*.

#### Equations governing and numerical simulation

The governing equations for the fluid flow field of the current problem are continuity (1) and Navier-Stokes equations (2) equations that are described as follows, respectively[13-15]:

(1) [Please see supplementary files to access the formulas.]

---

(2)

where  $u_i$ ,  $p$ , and  $\nu$  represent the velocity field, pressure, density, and kinematic viscosity, respectively.

Because of the presence of diffusers and holders in the ASRA exposure chamber, the flow is turbulent. Hence,  $\kappa$ - $\epsilon$  turbulence model was used to model the Reynolds stresses. The  $\kappa$ - $\epsilon$  model is one of the most widely used and proper two-equation turbulence models that has satisfactory accuracy and good stability for modeling. Also, because of its low computational cost, this model is widely used for turbulent flows [13]. The transport equations for turbulent kinetic energy (3) and the energy dissipation rate (4) are as follows, respectively:

(3) [See supp. files]

(4)

where  $G_k$  represents turbulent kinetic energy,  $G_b$  represents kinetic energy production, and  $C_{1\varepsilon}$  and  $C_{2\varepsilon}$  indicate constant coefficients.  $\sigma_k$  and  $\sigma_\varepsilon$  are the Prandtl number for  $\kappa$  and  $\varepsilon$ , respectively. The Prandtl number and constants are determined as follows:

[See supp. files]

To drawing of geometries, meshing of the field, and solving of equations, respectively, *Design Modeler*, *ANSYS Meshing*, and *ANSYS FLUENT* software in the *ANSYS Workbench18* package were used. The governing equations in three-dimensional (3D) were solved, and the *SIMPLE* algorithm was employed for coupling the velocity and pressure. The *Pressure-based* finite volume method was used to discretize the governing equations of the continuous phase. To model the particles, the *Discrete Phase Model* (DPM) was used. *Velocity-inlet*, *Pressure-outlet* and *Stationary wall (no-slip)* were defined as boundary conditions, for inlet, outlet and walls, respectively. To validate the presumption numerical model, the experimental results of Chen *et al.* study were compared with the results of numerical simulation [13, 15].

#### Meshing and determining the optimal grid

In numerical simulation, the structure and quality of the created computational grid have a great impact on the convergence, correctness, and accuracy of the results. In the current study, based on the matrix of experiments, five-chamber designs were introduced and different grid resolutions of the computational domain were generated by *ANSYS Meshing* software. Size of the grid became finer at the boundaries of the chamber to guarantee the accuracy of computations. At least five coarse to fine grids were created for each chamber design and the independence of the numerical results from the generated grid was studied. The optimal grid is the point where, as the grid becomes finer, there is no noticeable change in the numerical resolution accuracy, and the variable graphs under consideration at this point almost overlap. From the last two graphs, a graph with fewer elements introduces an optimal grid, it has accuracy and optimal computational cost.

The quality of the meshing was confirmed using minimum orthogonal quality. The used variable for the study of the independence of the grid was the average weighted velocity of the flow along the radius of the chamber at 110 cm distance to the chamber opening (inlet).

#### Particle Sampling

After numerical simulation of the matrix of experiments, *CFD-Post* software was used to sample the concentration of particles in the respiratory zone of the studied animals. A total of 40 points were determined for particle concentration sampling. These points were located above the animal's respiratory zone at the opening of each holder on a surface ending in the central axis of the chamber. The MPC was then calculated for each holder, and finally for each design of the matrix. The results (MPC) were entered in DE7 software as response variables and analyzed.

## Results

### Matrix of experiments

Due to the presence of four independent factors for the design of experiments (chamber height, carrier gas density, particle aerodynamic diameter, and particle inlet concentration), a total of 30 design of experiments were introduced by DE7 software. Based on the information of this matrix, five types of chamber geometries with five heights and with their specific flow characteristics were introduced. These designs were drawn for the heights of 1, 1.5, 2, 2.5, and 3 times the radius of the cylinder section, namely D1 to D5, respectively.

### Drawing geometry, meshing and determining the optimal grid

Because the chamber's geometry had axial symmetry, only a quarter of the geometry and its components were drawn and meshed with two symmetrical plates to reduce the cost and time of numerical computations. The dimensions of the chambers, the number of nodes of the optimized grid and the quality of mesh are presented in Table 1.

**Table 1.** properties of the five-design of chambers and their optimized computational grids

<i>D5</i>	<i>D4</i>	<i>D3</i>	<i>D2</i>	<i>D1</i>	Cod of the chamber
227.41	209.41	191.41	173.41	155.41	Length X (cm)
36	36	36	36	36	Length Y,Z (cm)
108	90	72	54	36	Height of the cylinder of the chamber (cm)
1.5675e+5	1.3843e+5	1.201e+5	1.0178e+5	8.3460e+4	Volume (cm <sup>3</sup> )
7.46e+5	6.72 e+5	8.80 e+5	9.12e+5	9.3 e+5	Number of the Nods
0.67	0.74	0.76	0.73	0.65	Orthogonal quality

### Validation of the presumption numerical model

The experimental results of the study of Chen et al. were used to examine and confirm the numerical presumption model [13]. In Fig1, the changes of the x-component of velocity and the normalized concentration of the particles have plotted at the mid-section of the chamber along with the lines  $x = 0.4$  and  $0.6$ , (experimental and CFD results). Matching of the curves shows that the numerical model has satisfactory accuracy to predict the velocity field and particle concentration in the reference chamber; in

other words, the presumption model has adequate validity to trace particles in the similar geometries like ASRA inhalation exposure chamber.

### Numerical simulation and analysis

Numerical simulation of the matrix of experiments was performed by the validated numerical model. The values of response variables (*mean particle concentration in the respiratory zone of the animal*) for each design of the experiment were obtained in the post-processing stage, and their corresponding results were entered in DE7 software.

### Factors screening, mathematical modeling, and optimizing

The primary data analysis was performed by DE7 to screen for factors and determine the predictive mathematical model of mean particle concentration in the respiratory zone of the animal. In the *fit summary* step, the linear model (2FI) was significant ( $P < 0.05$ ) and suggested. The 2FI model was significant with the presence of the inlet particle concentration and the aerodynamic diameter of the particles (Equation 5). The results of the analysis of variance for the model are presented in Table 2.

$$C_2 = 0.8757 (C_1) + 0.0083 (d_A) - 0.013685 (d_A)(C_1) + 0.12023 \quad \text{(Equation 5)}$$

In Equation 5 and Table 4,  $C_1$  ( $\text{mg}/\text{m}^3$ ) represents the inlet particle concentration,  $C_2$  ( $\text{mg}/\text{m}^3$ ) represents the mean particle concentration in the respiratory zone of the animals, and  $da$  ( $\mu\text{m}$ ) represents the aerodynamic diameter of the particles.

**Table 2.** The analysis of variance of the 2FI model

	Sum of square	Mean square	Degree of freedom (df)	<i>p.value</i>
dA ( $\mu\text{m}$ )	47.94	28.32	1	<0.0001
$C_1$ ( $\text{mg}/\text{m}^3$ )	6220.32	3674.28	1	<0.0001
Interaction dA and $C_1$	16.10	16.01	1	<0.0001

The 2FI model has an *R-squared* of higher than 99.5%, *adjusted R-squared* of 99.34% and *predicted R-squared* of 99.17%. To optimize the chamber's height and to determine its permissible range, the uniformity of the particle distribution in the chambers of different heights was analyzed using the ANOVA. The results showed that in the D3 and D4 designs of chambers, the mean particle concentration in the openings of the holders did not differ significantly ( $P > 0.05$ ) but this index was statistically significant in the other three chambers (D1, D2, and D5). In other words, the permissible range of height tolerance that resulted in uniform distribution of particles in these chambers was 2-2.5 times the radius of the chamber's cylindrical section.

The effect of the simultaneous changes of the independent variables on the response variable (MPC) can be seen in the 3D graph of Fig 2. At values close to the low range of the mean inlet concentration, the change in the aerodynamic diameter of the particles (in the defined range) has very little effect on the response variable, but at near-high values of it, with raising aerodynamic diameter of the particle, it has a greater effect on the response variable.

## Discussion

In the current study, optimizing the geometry of the ASRA exposure chamber was done, the effective factors on its performance were screened. For the first time, a mathematical model was introduced to estimate the MPC. The results indicated that in the optimized chamber, the flow in the respiratory zone of the studied animals was developed and the path lines became parallel with no eddy flows. Therefore, the stability and uniform distribution of the particle concentration in the target zone are ensured during the test duration. The uniform distribution of TM in the respiratory zone of the studied subjects is an important criterion for validating studies on the toxicology of suspended particles [7, 16, 4, 2]. So far many inhalation exposure chambers have been designed and used, but in most cases, variations in the concentration of the TM have been observed in the target zones[2]. In the current study, to achieve a developed flow and uniform distribution, the height of the chamber cylindrical section was optimized as the most important factor of the geometry domain. The results showed that in chambers with a height less than 2 or over 2.5 times radius of the cylindrical section, the  $MPC_s$  were significantly different. In other words, the permissible height is 2–2.5 times the radius of the cylindrical section. To examine the concentration changes in previous chambers, the chamber designed by Barrow *et al.* could be mentioned. The evaluation of this chamber's performance was carried out using the propylene glycol aerosol with 24 empty cages without laboratory animals. The chamber was designed to expose 48 rats in two sections and one level. The aerosol concentration gradient inside the chamber varied between 55% and 99% of the concentration of the inlet atmosphere [17]. One drawback of Barrow *et al.*'s study is the absence of laboratory animals in the chamber when concentrations were being evaluated. Any obstacle to the flow's direction can cause flow turbulence so that the presence or absence of the animal cannot be considered the same. However, the design of the chamber was so poor that even without the presence of the animals, a large gradient of concentration was reported in the results. Of course, another important factor that led to a sharp variation of concentration in the Barrow's chamber is the direction of flow that was designed horizontally. In the present study, these defects were corrected and optimization and evaluation of the chamber performance were performed with the presence of the animals in the chamber. Also, Cheng *et al.* studied the performance of the H2000 and H1000 chamber and showed variations in the concentrations of particles with a mean diameter of 1.6 and 3.1  $\mu\text{m}$  were 4.5–12.6% and 7.7–46.3%, respectively [18]. The gradients of particle concentration in these two types of chambers are high, and one of its causes is the design of 3 levels for animal exposure inside the chamber. The optimized chamber in the current study has a level for exposure, and the placement of the animal holders in the chamber is also symmetric, and there was no significant difference in mean concentrations among the respiratory zones of the animals. Besides, O'Shaughnessy *et al.* designed a chamber with 8 sections and two exposure levels [19]. In this chamber design, two levels of exposure and the horizontal flow raised the concentration variation in the chamber. The studies of O'Shaughnessy *et al.* and Cheng *et al.* showed that with raising particle's mean aerodynamic diameter, the variation in the particle concentration inside the exposure chamber increased, leading to the delivery of unequal doses to the members of the studied group [19, 18].



The designs of chambers that have so far been presented have not addressed optimization and modeling to predict PCM in the respiratory zone of the under study animals. The most important reason for not implementing it was the multilevel location of animals in some chambers and the instability of particle concentrations in different areas of the exposure chambers. The design of single-level exposure and fixation of animals at specified locations (holders) in the ASRA chamber allowed the optimization and mathematical modeling of the chamber. Another factor in the ASRA exposure chamber's design that has not been observed in the above-cited studies is the axial symmetry in the chamber geometry that could create a uniform distribution of particles after the development of flow in the cylindrical section[9]. Until now, the exposure zones in all chambers have been designed as a polygon that is less symmetrical than circular cross-sections and in which particle concentration distribution is less uniform.

In the current study, after optimizing the geometry and determining the permissible range of the height of the cylindrical section of the chamber, the needed statistical analysis was performed and according to statistical indices, the linear model (2FI) was chosen. The factors effective on the response variable in the final model were the inlet concentration, the aerodynamic diameter ( $d_a$ ) of the particles, and their interaction. Based on the results of data analysis, the height and density of carrier gas in the determined range did not affect the response variable (MPC) and were removed. The coefficients of recognition (R-squares) of the model are over 99% which shows that the 2FI model is highly capable of predicting the response variable.

## Conclusion

A uniform and stable distribution of the test material in the respiratory zone of the subject under study is a key factor for designing and using IECs. uniform and stable distribution of the test material in the respiratory zone of the subject under study is a key factor for designing and using IECs. Considering the advantages and disadvantages of the previous chambers' designs in designing of the ASRA chamber and geometry optimization helped to create a uniform and stable distribution of MPC and enabled the development of a mathematical model for predicting MPC. The 2FI model obtained is specific to the ASRA chamber and can also enable users to easily and reliably calculate the MPC in the target zone without experimental sampling. It is suggested that, given the development of nanoparticles in today's societies, a study be conducted to optimize and model the ASRA chamber for nanoparticles at the applicable practical concentrations.

## Abbreviations

IEC: Inhalation Exposure Chamber; TM: Test Atmosphere; MPC: Mean Particle Concentration; 2FI: Two Factor Interaction;  $d_a$ : Aerodynamic Diameter of the Particles

## Declarations

### Ethical approval and consent to participate

Not applicable

### **Consent for publication**

Not applicable

### **Availability of supporting data**

The datasets analyzed are not publicly available, but are available from the corresponding author on reasonable request, after approval by Tarbiat Modares University as the sponsor.

### **Competing interests**

The authors declare that they have no competing interests

### **Funding**

The current study was funded by Tarbiat Modares University, Tehran, Iran.

### **Authors' contributions**

Conceptualization: H. Rajabi-Vardanjani and H. Asilian-Mahabadi; formal analysis: M. Sedehi; data collection: H. Rajabi-Vardanjani and M. Bayareh; writing—original draft preparation: H. Rajabi-Vardanjani; Writing-review and editing, H. Asilian-Mahabadi, M. Bayareh, M. Sedehi; funding acquisition: H. Rajabi-Vardanjani and H. Asilian-Mahabadi. All authors read and approved the final manuscript.

### **Acknowledgements**

The authors thank Tarbiat Modares University as the sponsor of this study.

### **Authors' information**

Hassan Rajabi-Vardanjani<sup>1</sup>, Hassan Asilian-Mahabadi<sup>1\*</sup>

*<sup>1</sup>Department of Occupational Health Engineering, Faculty of Medical Sciences, Tarbiat Modares University, Tehran, Iran.*

Morteza Bayareh<sup>2</sup>

*<sup>2</sup>Department of Mechanical Engineering, Faculty of Engineering, Shahrekord University, Shahrekord, Iran.*

Morteza Sedehi<sup>3</sup>

*<sup>3</sup>Department of Epidemiology and Biostatistics, School of Public Health, Shahrekord University of Medical Sciences.*

# References

1. Yi J-S, Jeon K-S, Kim H-J, Jeon K-J, Yu I-J. Development of a Nose-only Inhalation Toxicity Test Chamber That Provides Four Exposure Concentrations of Nano-sized Particles. *JoVE (Journal of Visualized Experiments)*. 2019(145):e58725.
2. Rajabi-Vardanjani Hassan, Asilian-Mahabadi Hassan, Morteza S. Particulate Matter Inhalation Exposure Chambers and Parameters Affecting Their Performance: A Systematic Review Study. *Health Scope*. 2019;8(4). doi:10.5812/jhealthscope.80163.
3. Karanasiou A, Viana M, Querol X, Moreno T, de Leeuw F. Assessment of personal exposure to particulate air pollution during commuting in European cities—Recommendations and policy implications. *Science of the Total Environment*. 2014;490:785-97.
4. Chen LC, Lippmann M. Inhalation toxicology methods: the generation and characterization of exposure atmospheres and inhalational exposures. *Current protocols in toxicology*. 2015;63(1):24.4.1-4.3.
5. Yi J, Chen BT, Schwegler-Berry D, Frazer D, Castranova V, McBride C et al. Whole-body nanoparticle aerosol inhalation exposures. *JoVE (Journal of Visualized Experiments)*. 2013(75):e50263.
6. ASHRAE A, editor. *ASHRAE Handbook-HVAC Applications*. American Society of; 2011.
7. Kimmel EC, Yerkes KL. Performance, fluid mechanics, and design of a small-animal, whole-body inhalation exposure chamber. *Inhalation toxicology*. 1997;9(3):287-316.
8. Oldham MJ, Phalen RF, Robinson RJ, Kleinman MT. Performance of a portable whole-body mouse exposure system. *Inhalation toxicology*. 2004;16(9):657-62.
9. Rajabi-varlanjani H. *Designing, Optimization, and Modeling of the Inhalation Dust Exposure Chambers Using Computational Fluid Dynamics and Assessing the Final Analytic Model by The Experimental Method*. Iranian Research Institute for Information Science and Technology: Tarbiat Modares University; 2019.
10. Löndahl J, Massling A, Pagels J, Swietlicki E, Vaclavik E, Loft S. Size-resolved respiratory-tract deposition of fine and ultrafine hydrophobic and hygroscopic aerosol particles during rest and exercise. *Inhalation toxicology*. 2007;19(2):109-16.
11. Council NR. *Guide for the care and use of laboratory animals*. National Academies Press; 2010.
12. Durakovic B. Design of experiments application, concepts, examples: State of the art. *Periodicals of Engineering and Natural Sciences*. 2017;5(3).
13. Chen F, Simon C, Lai AC. Modeling particle distribution and deposition in indoor environments with a new drift-flux model. *Atmospheric Environment*. 2006;40(2):357-67.
14. Rodi W. *Turbulence models and their application in hydraulics*. Routledge; 2017.
15. *Guide AFUs*. Release 17.0. Ansys Inc. 2016.
16. Morency F, Hallé S. Modelling nanoparticle transport in an animal exposure chamber: a comparison between numerical and experimental measurements. *WIT Transactions on Engineering Sciences*. 2010;69:533-43.

17. Barrow CS, Steinhagen WH. Design, construction and operation of a simple inhalation exposure system. *Fundamental and Applied Toxicology*. 1982;2(1):33-7.
18. Cheng Y-S, Barr EB, Carpenter RL, Benson JM, Hobbs CH. Improvement of aerosol distribution in whole-body inhalation exposure chambers. *Inhalation Toxicology*. 1989;1(2):153-66.
19. O'Shaughnessy PT, Achutan C, O'Neill ME, Thorne PS. A small whole-body exposure chamber for laboratory use. *Inhalation toxicology*. 2003;15(3):251-63.

## Figures

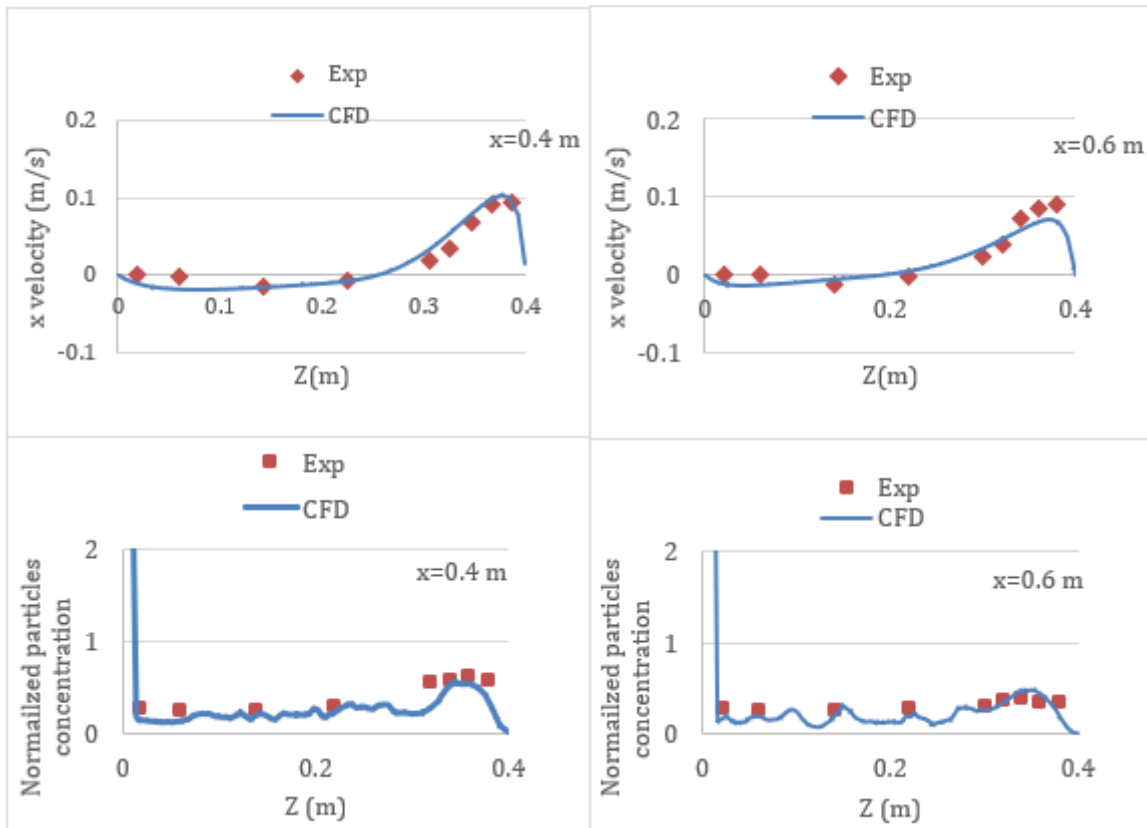


**Figure 1**

The changes of the x-component of velocity and the normalized particles concentration at the mid-section of the chamber (experimental and CFD).

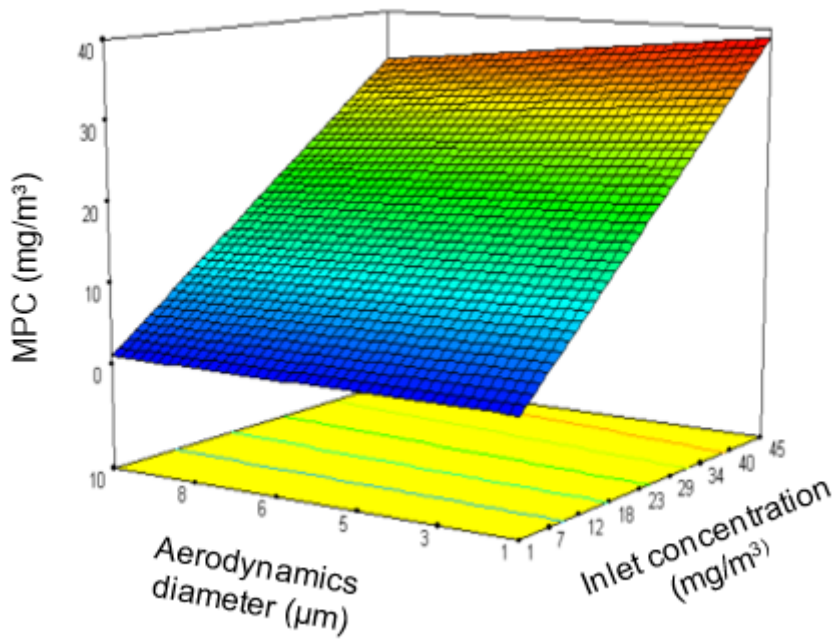


**Figure 2**

3D graph of the simultaneous changes of the independent variables on the MPC

## Supplementary Files

This is a list of supplementary files associated with this preprint. Click to download.

- [Formulas.docx](#)